An explanation of the observed excess emissions in our galaxy using the Axion Quark Nugget dark matter model

Michael Sekatchev*
Department of Physics and Astronomy, University of British Columbia
6224 Agricultural Road, Vancouver, British Columbia, Canada, V6T 1Z1
(Dated: December 10, 2022)

Telescope observations of background radiation in the Milky Way point to an anomalous excess in ultraviolet, microwave, and radio signals. The novel Axion Quark Nugget (AQN) dark matter model may provide an interpretation for this as-yet-unexplained excess. Baryonic matter in the galaxy may collide with antimatter AQNs and annihilate, resulting in an emission of a broad spectrum of electromagnetic radiation similar in form to Bremsstrahlung. We propose to perform the comparison of AQN annihilation radio emissions with the observed radio haze from WMAP. Understanding the source(s) of the excess radiation in our galaxy may bring us a step closer to revealing the exact nature of dark matter.

I. MOTIVATION

An observation of the Cosmic Microwave Background (CMB) was reported in the first year of data from the Wilkinson Microwave Anisotropy Probe (WMAP), which collected full-sky observations of the microwave radiation in five frequency bands (23 to 94 GHz) [1]. The collected data was contaminated with a microwave foreground from both Galactic emission and extragalactic point sources. The foreground Galactic emissions were modelled with three components: synchrotron, free-free, and dust emission [2]. These were used in combination with the data from the five frequency bands to isolate the CMB. The models were useful for reducing the CMB data contamination from Galactic emission as a whole, but were not particularly physical and could only weakly distinguish between the three individual emission components.

Finkbeiner 2004 proposed an alternative interpretation for the three components and subtracted the fits of each from the WMAP's Galactic emission data [6]. The remainder was an excess signal at each of the five bands, termed the WMAP "haze". An excess has also been observed in the ultraviolet (UV) Galactic signals by the GALEX telescope [11], and in the x-ray by three independent observations [8].

Many explanations for the excess in these bandwidths were proposed, including annihilation or decay within the Weakly Interacting Massive Particle (WIMP) dark matter model ([7], [14], [4] for radio, [11] for UV). It was found that the mass of the WIMPs would need to be ~ 100 GeV to obtain the necessary signature. The existence of WIMPs with the required mass has been ruled out by dark matter detection experiments [10]. If instead the central value of the WIMP mass is used, the signal is below the observed intensity [3]. In the case of UV emissions, for instance, the estimates from the WIMP model are 12 orders of magnitude lower than the signal observed by GALEX: $10^{-17}\,\mathrm{erg\,cm^{-2}\,s^{-1}}$ versus the expected $10^{-5}\,\mathrm{erg\,cm^{-2}\,s^{-1}}$ [11].

We propose that an annihilation interaction within the Axion Quark Nugget (AQN) model may provide an explanation for the observed excess in these bandwidths. The model proposes that dark matter is dominated by macroscopic composite objects of nuclear density, in the form of matter and antimatter nuggets [20]. The antimatter nuggets consist of a core from antiquarks in the color superconducting phase, immersed in a positron-sphere to ensure the antinugget's electrical neutrality. Because of their large mass ($\sim 10^0 - 10^3$ g), the nuggets have a low number density, making direct detection statistically impossible and detection through an electromagnetic interaction unfeasible.

Baryons originating mainly from the ionized gas in the Warm Hot Intergalactic Medium (WHIM) surrounding the Milky Way may collide with antimatter AQNs and annihilate. Part of the available 2 GeV of energy is used to heat the antinugget's positron-sphere, and is radiated away. The resulting spectrum was estimated to match the excesses in radio [9], UV [21], and x-ray [8] signals in the galaxy.

We propose to compare the AQNs' annihilation interactions' radio emissions with the observed radio haze from Planck and WMAP [9], building onto the initial estimate by using numerical integration to determine the flux from this interaction in all directions. This flux will be used to produce sky maps of the expected signal which can be directly compared to telescope observations. This requires models of local baryon gas and dark matter number density distributions in the Milky Way, both of which are available [18] [15]. The results of this comparison will be used to obtain an improved estimate of the mean AQN mass, and eventually extended to constraints on a realistic AQN mass distribution.

If successful, our proposal will provide strong evidence for the nature of dark matter in the form of Axion Quark Nuggets as well as explain the observed excesses in emissions in our galaxy.

*Electronic address: michaelsekatchev@live.ca

II. THEORY

Here we examine the equations for the AQNs' emissivity, as well as the baryon and dark matter number density distributions, which will be used in the analysis.

A. AQN Emissivity

An analytic estimate of the spectral surface emissivity of a single AQN is given in [9]:

$$\begin{aligned}\frac{\mathrm{d}F}{\mathrm{d}\omega}(\omega) &= \frac{\mathrm{d}E}{\mathrm{d}t\mathrm{d}A\mathrm{d}\omega} \\ &\sim \frac{4}{45}\frac{T^3\alpha^{\frac{5}{2}}}{\pi}\sqrt[4]{\frac{T}{m_e}}\left(1+\frac{\omega}{T}\right)e^{-\frac{\omega}{T}}h\left(\frac{\omega}{T}\right),\end{aligned} \tag{1}$$

where T is the nugget's temperature, α is the fine structure constant, m_e is the mass of an electron, and $h(x)$ is

$$h(x) = \begin{cases} 17 - 12\ln(x/2), & x < 1 \\ 17 + 12\ln(2), & x \geq 1. \end{cases} \tag{2}$$

Equation (1) can be integrated over ω to find the total flux emitted per area $\mathrm{d}A$ of the nugget's surface,

$$F_{\mathrm{tot}} = \frac{\mathrm{d}E}{\mathrm{d}t\mathrm{d}A} = \int_0^\infty \mathrm{d}\omega \frac{\mathrm{d}F}{\mathrm{d}\omega}(\omega) \approx \frac{16}{3}\frac{T^4\alpha^{\frac{5}{2}}}{\pi}\sqrt[4]{\frac{T}{m_e}}. \tag{3}$$

The nugget is assumed to be in thermal equilibrium. This means that the rates of emission and annihilation must be balanced. If only a fraction $1-g$ of the energy is thermalized, we have

$$F_{\mathrm{tot}} = (1-g)\,F_{\mathrm{ann}} = (1-g)\frac{\mathrm{d}E_{\mathrm{ann}}}{\mathrm{d}t\mathrm{d}A}, \tag{4}$$

where F_{ann} is the rate of annihilation,

$$F_{\mathrm{ann}} = 2\,\mathrm{GeV}\cdot f\cdot v\cdot n_{\mathrm{bar}}\left(\vec{\mathbf{r}}\right). \tag{5}$$

Here $2\,\mathrm{GeV} = 2m_p$ is the energy released by proton annihilation, v is the relative speed between dark matter and visible matter, $n_{\mathrm{bar}}\left(\vec{\mathbf{r}}\right)$ is the local baryon density, and f is a factor accounting for the possibility of reflection instead of annihilation [8]. By substituting (3) and (5) into (4), an analytic expression for the nugget temperature is determined:

$$T = \left[\frac{3}{16}\pi(1-g)(2\,\mathrm{GeV})\,f\,v\frac{1}{\alpha^{5/2}}m_e^{1/4}(n_{\mathrm{bar}}(\vec{\mathbf{r}}))\right]^{4/17}. \tag{6}$$

Having obtained the nugget temperature using (6), we are now able to calculate the spectral surface emissivity for an AQN at any point in the galaxy using (1). The flux obtained from equation (1) is for an element of area $\mathrm{d}A$ on the nugget surface, and needs to be converted to the flux for a local volume element $\mathrm{d}V$ in the galaxy. This involves first integrating over the nugget's surface, which adds a factor of $4\pi R_{\mathrm{AQN}}^2$ (where R_{AQN} is the nugget's radius), to obtain the total emissivity of a single AQN, and then multiplying by the local dark matter number density $n_{\mathrm{DM}}\left(\vec{\mathbf{r}}\right)$. The spectral spatial emissivity is therefore

$$\mathrm{d}\epsilon_\omega = \frac{\mathrm{d}E}{\mathrm{d}t\mathrm{d}V\mathrm{d}\omega} = \frac{\mathrm{d}F}{\mathrm{d}\omega}(\omega)\cdot 4\pi R_{\mathrm{AQN}}^2\cdot n_{\mathrm{DM}}. \tag{7}$$

The numerical integration the local spectral spatial emissivity elements along sightlines will be used to create sky maps of the expected signal from AQN annihilations in all directions.

We see that (7) has a dependence on the dark matter number density $n_{\mathrm{DM}}\left(\vec{\mathbf{r}}\right)$. It can be seen in (6) that the nugget temperature has a dependence on the local baryon number density $n_{\mathrm{bar}}\left(\vec{\mathbf{r}}\right)$. This means that the local spectral spatial emissivity elements $\mathrm{d}\epsilon_\omega$ depend on both the local dark matter and the baryon number densities. Proposed models for both are described in the sections that follow.

As an additional element in our study, we will also account for ionization of the AQNs. If the temperature of gas components in the galaxy exceeds $3\cdot 10^4$ K, they are treated as ionized [18]. The AQNs can also become ionized as a result, which increases their effective capture radius from their neutral form. A larger capture radius will result in an increase in annihilations and therefore emissions, as can be seen in (7). The exact relationship between the effective capture radius R_{eff} and the temperature of the nugget T and surrounding gas T_{gas} is obtained from [16] as

$$R_{\mathrm{eff}} = \frac{R_{\mathrm{AQN}}^2}{T_{\mathrm{gas}}}\sqrt{\frac{8m_e}{\pi}T^3}. \tag{8}$$

This currently being verified to ensure that it applies for low AQN temperatures and baryon number densities.

B. Baryon Number Density – Gas-Halo

The natural first choice for a Milky Way visible and dark matter mass density model was the standard Disk-Bulge-Halo (DBH) model based on a variety of observational data, described in [19] or [12]. However, the gas components of DBH models are subject to the missing baryon problem: Big bang nucleosynthesis and observations of the CMB have determined the baryonic density parameter in the early universe to be $\Omega_b \approx 0.04$ [5]. The number of observed baryons only account for less than half of that amount [17].

To account for the missing baryons at high Galactic latitude, matter mass density models from [18] were used instead, which were produced from a simulation of a Milky Way-like galaxy. More specifically, [18] studies the properties of gas using three realistic simulations of

galaxies analogous to the Milky Way. We use the matter distribution from Eris2k (E2K), the latest of the three simulations. Although spherically symmetric, the paper provides a distribution of the mass density of four gas components against distance from the Galactic centre for E2K, shown in FIG. 1. These include cold neutral gas, warm gas, warm-hot gas and hot gas.

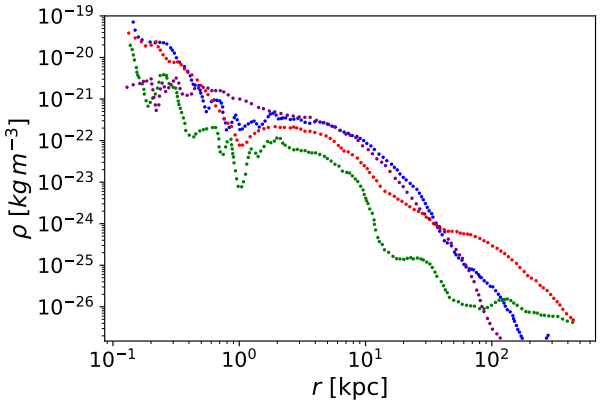

FIG. 1: Mass density distributions of the four hydrogen gas components from the Eris2k Milky Way-like galaxy simulation [18]. The cold neutral gas component is shown in blue ($T_{\rm gas} < 3 \cdot 10^4\,$K). The warm ($3 \cdot 10^4\,{\rm K} < T_{\rm gas} < 10^5\,$K), warm-hot ($10^5\,{\rm K} < T_{\rm gas} < 10^6\,$K), and hot ($T_{\rm gas} > 10^6\,$K) ionized gas components are shown in green, red, and purple respectively. Each distribution will be fit to a sum of power functions and divided by the hydrogen mass to obtain the local ionized and neutral gas number densities in the entire galaxy. These will be used in the calculation of local spectral spatial emissivities within the Axion Quark Nugget annihilation interaction, which will be integrated to determine the flux contributions of this interaction to the observed radio signal in all directions.

We propose to fit each hydrogen gas component of the discrete E2K mass density distribution to a sum of five power functions,

$$\rho_{\rm gas}\left(\vec{\mathbf{r}}\right) = \rho_{\rm crit} \sum_{i=1}^{5} a_i \left(1 + \left(\frac{x}{b_i}\right)^2\right)^{-c_i}, \qquad (9)$$

each of which is described by three parameters a_i, b_i, and c_i. Here $x = r/r_{\rm vir}$ where $r = |\vec{\mathbf{r}}|$ and $r_{\rm vir} = 233$ kpc is the virial radius of E2K [18].

C. Dark Matter Number Density – NFW-Halo

An Navarro–Frenk–White (NFW) profile was used for modelling the dark matter mass density in the Milky Way [15], a common choice in cosmological simulations involving only dark matter. The NFW halo was modelled as:

$$\rho_{\rm DM}(\vec{\mathbf{r}}) = \frac{\rho_{0,\rm h}}{\left(\frac{r}{r_{\rm h}}\right)\left(1 + \frac{r}{r_{\rm h}}\right)^2} \qquad (10)$$

where $r = |\vec{\mathbf{r}}|$, $r_{\rm h}$ the scale radius, and $\rho_{0,\rm h}$ the scale density. The values for $r_{\rm h}$ and $\rho_{0,\rm h}$ are shown in Table 1, taken from [13], which improves and further constrains the parameters shown in the original study, [12].

TABLE I: Expectation values with uncertainties for the Navarro–Frank–White dark matter mass density profile (10). Summarized from [13].

Quantity	$r_{\rm h}$	$\rho_{0,\rm h}$
Unit	kpc	$M_\odot pc^{-3}$
Value	19.0 ± 4.9	0.0106 ± 0.0053

III. DETAILS ON PROPOSED COMPUTATION

A sky map of the expected radio signal from the AQN annihilation interaction will be created and compared to five bands of the WMAP haze shown in [6]. The data is publicly available (see section IV), and a half-sky Cartesian projection of the K-band is presented in FIG. 2.

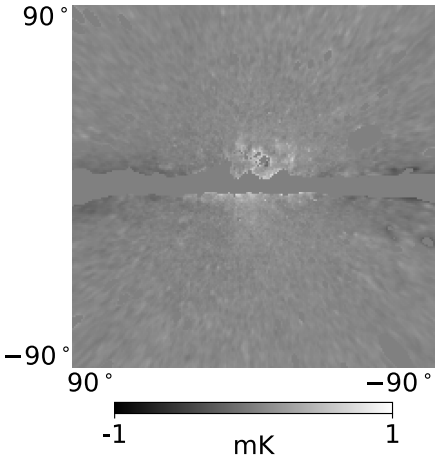

FIG. 2: Cartesian half-sky projection of the K-band component of the WMAP haze (23 GHz), created using Python's Healpy library with data from [6]. This signal was obtained in [6] as the remainder after subtracting models of all possible contributors to the sky signal observed by WMAP. The plot is in thermodynamic temperature units, stretched to fit in the range [-1 mK, 1 mK], which corresponds to ±15 Jy/sr. Bright point sources and a region in the plane where the signal is dominated by dust extinction are masked (8.9% of the projection). An identical sky map of the AQN annihilation signature at 23 GHz will be created and compared to this one in magnitude and signal distribution.

In order to create a sky map of the AQN annihilation radio emissions to compare with FIG. 1, we propose to

discretize the entire sky as seen from Earth's perspective into pixels, where each n-th pixel is defined in spherical coordinates, (θ_n, ϕ_n). In order to accomplish this, Python's Healpy library will be used (see section IV). Healpy contains the HEALPix scheme, which partitions a sphere into equal area quadrilaterals of varying shape. The flux observed at each pixel will be equal to the sum of the flux observed from each volume element $\mathrm{d}V$ from the origin to the edge of the Galaxy in the direction of that pixel. This amounts to performing a sightline integral along discrete distance elements $\mathrm{d}r$ ranging from 0 to the edge of the galaxy in that particular θ_n, ϕ_n direction. The hydrogen number density, $n_{\mathrm{bar}}(x_{ni}, y_{ni}, z_{ni})$, will be calculated for these points along the sightline, using the model described in section II B, shifted to be earth centric, rather than galaxy-centric. From this the local nugget temperature, $T_{\mathrm{AQN}}(x_{ni}, y_{ni}, z_{ni})$, will be calculated using the analytical equation (6). The spectral spatial emissivity will now be calculated at all points along the sightline using (7). The flux from each i-th element along the sightline is given by

$$\mathrm{d}F_{\omega,ni} = \frac{\mathrm{d}\epsilon_{\omega,ni}\mathrm{d}V_i}{4\pi r_i^2} = \frac{\mathrm{d}\epsilon_{\omega,ni} r_i^2 \mathrm{d}r_i \mathrm{d}\Omega}{4\pi r_i^2} = \frac{\mathrm{d}\epsilon_{\omega,ni}\mathrm{d}r_i\mathrm{d}\Omega}{4\pi}, \tag{11}$$

where we see that the solid angle $\mathrm{d}\Omega$ is the same for all pixels, Because the HEALPix discretization creates pixels of equal area. We sum up these contributions to obtain the flux for each n-pixel,

$$F_{\omega,n} = \sum_{i=0}^{i_{\max}(n)} \mathrm{d}F_{\omega,ni} = \sum_{i=0}^{i_{\max}(n)} \frac{\mathrm{d}\epsilon_{\omega,ni}\mathrm{d}r_i\mathrm{d}\Omega}{4\pi}, \tag{12}$$

which can be plotted on a sky map and compared to the projection in FIG. 2. Here $i_{\max}(n)$ is the last discretized element along a sightline for the n-th pixel.

An estimate of the average AQN mass will be obtained from the comparison of the radio signal from AQN annihilations to the observed WMAP haze using a χ^2 fit. This will later be extended to a Markov Chain Monte Carlo method to obtain constraints on the AQN mass distribution.

The calculation above will be modified to include ionized AQNs by summing the separate contributions to each $\mathrm{d}\epsilon_{\omega,ni}$ from the four gas components in FIG. 1.

IV. RESOURCES LIST

Initial computations and estimates were hosted on the UBC Physics and Astronomy department's Consus server. Access to the Canadian Advanced Network for Astronomical Research (CANFAR) Science Portal[1] has been obtained, and will be used moving forward. All computations are performed in Python, using Jupyter Notebook[2]. Within Python, the Healpy library[3] will be used for its HEALPix scheme for partitioning a sphere into pixels of equal area and for generating full-sky projections. The Astropy library[4] will be used for accessing the necessary physical constants for the project, performing dimensional analysis, and unit conversions. The WMAP haze data will be obtained from the source provided in [6][5], and other information about the satellite will be taken from the WMAP NASA's dedicated WMAP site[6].

V. PLANNED SCHEDULE

TABLE II: Schedule for completion of the project throughout the two-term PHYS 449 course.

Date	Deliverable
September	Familiarization with project
October	Research available WMAP Haze data, coding emissivity integration
November	Preparation of written and oral project proposal
December	E2K mass density fitting, AQN Radio emissivity estimate
January	AQN Radio emissivity estimate
February	Estimating average AQN mass and AQN mass distribution. Beginning of thesis writing
March	Thesis writing and talk preparation

[1] https://www.canfar.net/en/

[2] https://jupyter.org/

[3] https://healpy.readthedocs.io/en/latest/

[4] https://www.astropy.org/

[5] skymaps.info

[6] https://wmap.gsfc.nasa.gov/

[1] C. L. Bennett, M. Halpern, G. Hinshaw, N. Jarosik, A. Kogut, M. Limon, S. S. Meyer, L. Page, D. N. Spergel, G. S. Tucker, E. Wollack, E. L. Wright, C. Barnes, M. R. Greason, R. S. Hill, E. Komatsu, M. R. Nolta, N. Odegard, H. V. Peiris, L. Verde, and J. L. Weiland. First-year wilkinson microwave anisotropy probe (wmap) observations: Preliminary maps and basic results. *The Astrophysical Journal Supplement Series*, 148:1–27, 09 2003.

[2] C. L. Bennett, R. S. Hill, G. Hinshaw, M. R. Nolta, N. Odegard, L. Page, D. N. Spergel, J. L. Weiland, E. L. Wright, M. Halpern, N. Jarosik, A. Kogut, M. Limon, S. S. Meyer, G. S. Tucker, and E. Wollack. First-year wilkinson microwave anisotropy probe (wmap) observations: Foreground emission. *The Astrophysical Journal Supplement Series*, 148:97–117, 09 2003.

[3] A. Bottino, F. Donato, N. Fornengo, and S. Scopel. Upper bounds on signals due to WIMP self-annihilation: Comments on the case of the synchrotron radiation from the galactic center and the WMAP haze. *Physical Review D*, 77(12), jun 2008.

[4] Eric Carlson, Dan Hooper, Tim Linden, and Stefano Profumo. Testing the dark matter origin of the wmap-planck haze with radio observations of spiral galaxies. *Journal of Cosmology and Astroparticle Physics*, 2013(07):026, jul 2013.

[5] Planck Collaboration et al. Planck 2018 results. VI. Cosmological parameters. , 641:A6, September 2020.

[6] Douglas P. Finkbeiner. Microwave interstellar medium emission observed by the wilkinson microwave anisotropy probe. *The Astrophysical Journal*, 614:186–193, 10 2004.

[7] Douglas P. Finkbeiner. Wmap microwave emission interpreted as dark matter annihilation in the inner galaxy. 2004.

[8] Michael McNeil Forbes and Ariel R. Zhitnitsky. Diffuse x-rays: Directly observing dark matter? *JCAP*, 0801:023, 2008.

[9] Michael McNeil Forbes and Ariel R. Zhitnitsky. WMAP Haze: Directly Observing Dark Matter? *Phys. Rev.*, D78:083505, 2008.

[10] Stefano Giagu. Wimp dark matter searches with the atlas detector at the lhc. *Frontiers in Physics*, 7, 05 2019.

[11] Richard Conn Henry, Jayant Murthy, James Overduin, and Joshua Tyler. The mystery of the cosmic diffuse ultraviolet background radiation. *The Astrophysical Journal*, 798(1):14, dec 2014.

[12] Paul J. McMillan. Mass models of the Milky Way. *Monthly Notices of the Royal Astronomical Society*, 414(3):2446–2457, 06 2011.

[13] Paul J. McMillan. The mass distribution and gravitational potential of the Milky Way. *Monthly Notices of the Royal Astronomical Society*, 465(1):76–94, 10 2016.

[14] Matthew McQuinn and Matias Zaldarriaga. Testing the dark matter annihilation model for the Wilkinson Microwave Anisotropy Probe haze. *Monthly Notices of the Royal Astronomical Society*, 414(4):3577–3589, 07 2011.

[15] Julio F. Navarro, Carlos S. Frenk, and Simon D. M. White. The Structure of Cold Dark Matter Halos. *Astrophys. J.* , 462:563, May 1996.

[16] Nayyer Raza, Ludovic Waerbeke, and Ariel Zhitnitsky. Solar corona heating by axion quark nugget dark matter. *Physical Review D*, 98, 11 2018.

[17] J. Michael Shull, Britton D. Smith, and Charles W. Danforth. The Baryon Census in a Multiphase Intergalactic Medium: 30% of the Baryons May Still be Missing. *Astrophys. J.* , 759(1):23, November 2012.

[18] A. Sokołowska, L. Mayer, A. Babul, P. Madau, and S. Shen. DIFFUSE CORONAE IN COSMOLOGICAL SIMULATIONS OF MILKY WAY-SIZED GALAXIES. *The Astrophysical Journal*, 819(1):21, feb 2016.

[19] Lawrence M. Widrow and John Dubinski. Equilibrium disk-bulge-halo models for the milky way and andromeda galaxies. *The Astrophysical Journal*, 631(2):838–855, oct 2005.

[20] Ariel Zhitnitsky. Axion quark nuggets. dark matter and matter–antimatter asymmetry: Theory, observations and future experiments. *Modern Physics Letters A*, 36(18):2130017, may 2021.

[21] Ariel Zhitnitsky. The mysterious diffuse uv radiation and axion quark nugget dark matter model. *Physics Letters B*, 828:137015, 2022.